Liquid Crystals
Publication details, including instructions for authors and subscription information:
http://www.informaworld.com/smpp/title~content=t713926090

Diffraction grating in a holographic polymer dispersed liquid crystal based on polyurethane acrylate

EunHee Kim[a]; JuYeon Woo[a]; ByungKyu Kim[a]
[a] Dept. of Polymer Science and Engineering, Pusan National University, Busan 609-735, Republic of Korea

To cite this Article Kim, EunHee , Woo, JuYeon and Kim, ByungKyu(2007) 'Diffraction grating in a holographic polymer dispersed liquid crystal based on polyurethane acrylate', Liquid Crystals, 34: 1, 79 — 85

To link to this Article: DOI: 10.1080/02678290601020005

URL: http://dx.doi.org/10.1080/02678290601020005

Liquid Crystals, Vol. 34, No. 1, January 2007, 79–85

Diffraction grating in a holographic polymer dispersed liquid crystal based on polyurethane acrylate

EUNHEE KIM, JUYEON WOO and BYUNGKYU KIM*

Dept. of Polymer Science and Engineering, Pusan National University, Busan 609-735, Republic of Korea

(*Received 9 January 2006; in final form 31 July 2006; accepted 10 August 2006*)

Diffraction modes of holographic grating were fabricated with polyurethane acrylates of various monomers, and with various film compositions, irradiation intensities, cell gaps and reading angles. An optimum monomer composition, LC content and irradiation intensity were obtained in terms of diffraction efficiency. Of the two types of multifunctional acrylate examined, dipentaerythritol penta-/hexa-acylate (DPHPA) gave better diffraction efficiency than the trimethylolpropane triacrylate (TMPTA) throughout the monomer compositions tested. This was interpreted in terms of high elasticity of the high functionality monomer. The existence of an optimum irradiation intensity at fixed resin composition was interpreted in terms of optimum rate of cure. A monotonic increases of diffraction efficiency with cell gap and interbeam angle were also noted, implying that the grating was formed uniformly as visualized by scanning electron microscopy.

1. Introduction

Polymer dispersed liquid crystals (PDLCs) are of technological importance in the development of switchable windows, electro-optic shutters, displays and, most recently, switchable gratings [1–3]. The most versatile method for forming PDLC structures is the photoinitiated polymerization of an initially homogeneous mixture containing reactive monomers and liquid crystal molecules [4]. Recently, volume holography techniques have been applied to conventional PDLCs, fabricating the controlled architectures of phase separated LC domains [5–7]. This type of PDLC is known as a holographic polymer dispersed liquid crystal (HPDLC) [8–10].

HPDLCs lead to several interesting potential applications [11]; for example, LC birefringence optical switches and hologram LC combinations have been proposed for reconfigurable optical computing, and for beam steering in laser radar. LC dynamic holographic gratings have also been exploited as an approach to volume optical data storage [12, 13]. This HPDLC has the advantage of modulating refractive index, competitive price, wavelength selectivity, and ability for external modulation in volume hologram applications.

HPDLCs are prepared by causing interference between two coherent laser beams in a photosensitive monomer/liquid crystal (LC) mixture contained between two substrates coated with a conductive layer, typically of indium tin oxide (ITO) [14]. Upon irradiation, a photoinitiator contained within the mixture initiates a free-radical reaction, causing the monomer to polymerize [15]. As the polymer network grows, the mixture phase separates into polymer-rich and liquid crystal-rich regions. Refractive index modulation between the two phases causes light passing through the film to be scattered, in the case of a traditional PDLC, or diffracted in the case of a HPDLC. When an electric field is applied across the cell, the index modulation disappears and light passing through the film is unaffected. In a conventional PDLC, the intensity of the illumination is uniform over the sample being cured, therefore the LC droplets are randomly distributed throughout the film, and the droplets have random orientation. In a HPDLC, the interference of the two laser beams sets up periodic bright and dark fringes within the film. Since the polymerization rate is proportional to the square root of laser intensity in radical polymerization [16], polymerization occurs rapidly in bright regions and slowly in dark regions. During hologram recording, monomer diffuses into the bright regions and LC toward the dark regions [17]. So, with the progress of polymerization, polymer-rich and LC-rich areas are formed periodically and, consequently, periodic lamellae of LC domains separated by polymer walls are fabricated [18, 19].

These periodic structures of multi-layers have very promising optical properties since a specific component

---

*Corresponding author. Email: bkkim@pnu.edu

Liquid Crystals
ISSN 0267-8292 print/ISSN 1366-5855 online © 2007 Taylor & Francis
http://www.tandf.co.uk/journals
DOI: 10.1080/02678290601020005

of the incident light is refracted by the LC droplets due to the difference in the refractive indices of the polymer and LC. The diffraction efficiency depends absolutely on the interface uniformity between the LC and polymer layer. So the key parameter in controlling the refraction is the clean phase separation between polymer and LC layers.

We fabricated transmission type holographic PDLCs with variation of monomer and film composition, irradiation intensity, cell thickness and interbeam angle. The diffraction efficiency and angular selectivity were measured by rotating the sample every 0.5° (θ) from the Bragg angle. The morphology of the HPDLC film was investigated by scanning electron microscopy (SEM).

2. Experimental

The composite films were prepared from a homogeneous prepolymer syrup consisting of a urethane acrylate oligomer, the nematic LC (E7), and the reactive diluent, viz. trimethylolpropane triacrylate (TMPTA), dipentaerythritol penta-/hexa-acrylate (DPHPA), and *N*-vinylpyrrolidinone (NVP). Multifunctional monomers (TMPTA and DPHPA) have very high reactivity and give extensive crosslinking of polymer, whereas monofunctional NVP extends the chains at a much lower rate and gives a linear polymer. However, the use of monofunctional monomer is essential to reduce the viscosity of the oligomer/LC mixture to ensure homogeneity of the starting mixture. Rose Bengal (0.3 wt%) was used as photoinitiator for holographic recording with an Ar-ion laser (λ=514 nm), where *N*-phenylgycine (NPG, 1.8 wt%) was added as coinitiator.

Polypropylene glycol (PPG, M_n=2000, Korea Polyol) was dried at 80°C, 0.1 mm Hg for several hours until no more bubbling was observed. The chemical reagents isophorone diisocyanate (IPDI) and hydroxyethyl methacrylate (HEMA) were used without further purification. PPG, IPDI and DBTDL (0.03 wt% based on base PUs) were mixed and reacted at 80°C for 3 h to obtain NCO-terminated prepolymer. The reaction mixtures were then cooled to 45°C before HEMA was added to obtain HEMA-capped urethane acrylate oligomer [20].

Table 1 shows the basic formulations which were irradiated at various laser intensities at different cell gaps. The holographic recording system is schematically shown in figure 1. An Ar-ion laser (514 nm) is used as light source. Beams pass through a spatial filter, a beam expander, and are split into two of identical intensity. These two beams are passed through a collimator and the central portions are reflected from mirrors and impinge normally on the same side of the cell. The cell was constructed by sandwiching the urethane acrylate oligomer, reactive diluents (acrylate monomers), and LC mixture between two ITO-coated glass plates. The interference of the two beams established the periodic interference pattern according to Bragg's law. The intersection angles of the two beams outside the cell were varied at 40°, 50°, 60° and 70°. Reading of the gratings was accomplished by an Ar-ion laser beam (514 nm) positioned at the Bragg angle. The diffracted beam was detected by a photodiode detector. Diffraction efficiency was determined by dividing the diffracted beam intensity of the sample cell by the transmitted beam intensity of a blank cell.

3. Results and discussion

The diffraction efficiencies of the HPDLC films for various polymer compositions are given in figure 2. A multifunctional acrylate, either a triacrylate (TMPTA) or a pentacrylate (DPHPA), and a monofunctional NVP are used with a HEMA-capped polyurethane oligomer to give the oligomer/TMPTA/NVP and oligomer/DPHPA/NVP systems. Through figures 2 (*a*, *b*, *c*), the NVP content is increased from one to three parts based on the 14 parts of polymer composition.

It can be seen that the diffraction efficiencies of the pentacrylate system are greater than those of the triacrylate system throughout the compositions tested, although both systems exhibit a maximum, which is over 80% for the pentacrylate at composition 4/5/1 and about 60% for the triacrylate system at 2/7/1.

Table 1. Formulation for Preparation of HPDLCs.

Prepolymer	LC content/wt%	Rose Bengal/wt%	NPG/wt%	Cell space/μm	Laser intensity/mW cm^{-2}
Oligomer/DPHPA (TMPTA)/NVP					10
	25			4.2	20
	30			7.9	30
	35	0.3	1.8	9.8	40
	40			11	50
	45			14	60
					80
					100

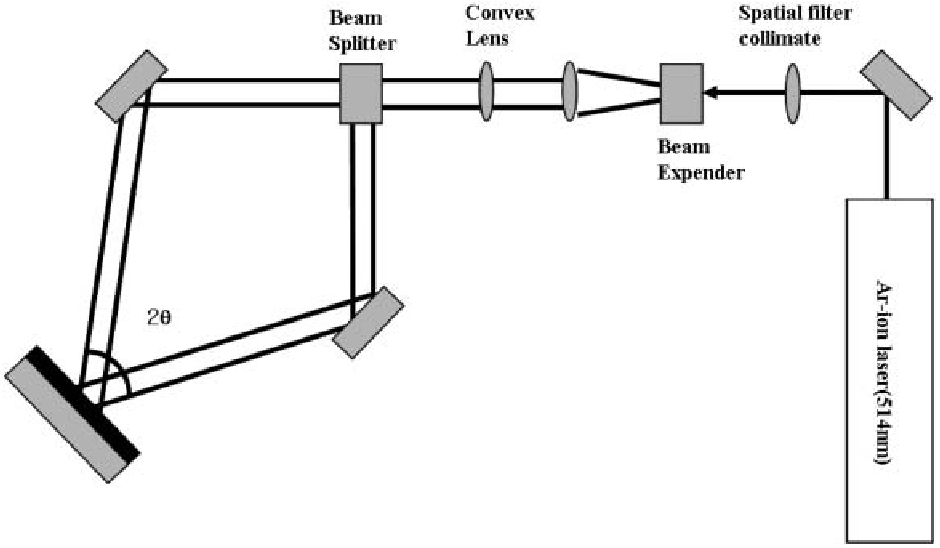

Figure 1. Experimental set-up for transmission mode HPDLCs.

As the monofunctional NVP content increases figures 2 (*a*→*c*), diffraction efficiency decreases [21]. Diffraction in a HPDLC is based on the difference in refractive indices between polymer and LC domains, i. e. the perfection of phase separation governs the diffraction efficiency. On the other hand, polymer–LC phase separation depends on the rate of cure and rate of diffusion, i.e. the migration of LC molecules from polymer-rich to LC-rich domains. When the rate of cure is too slow, neither significant networks nor migration of LC molecules are expected. When the rate of cure is too fast, diffusion may not take place and LC molecules are trapped within the polymer-rich domains. This leads to poor polymer–LC phase separation and low diffraction. Only at a reasonably high rate of cure, which is controlled by the irradiation intensity and monomer functionality [22, 23], does diffusion follow the reactions leading to gratings formation. As the acrylate monomers are consumed by the irradiation cure, concentration gradients of monomers as well as LCs are established perpendicular to the grating direction, leading to counter diffusions of monomer and LC molecules [24]. This type of diffusion is a molecular diffusion, which is governed by Fick's second law of diffusion [25]:

$$\frac{\partial C_{\mathrm{A}}}{\partial t} = D_{\mathrm{AB}}\underline{\nabla} C_{\mathrm{A}} \tag{1}$$

where C_{A}, D_{AB} and t are molar concentration of component A, binary diffusivity and time, respectively.

This type of molecular diffusion is driven by the consumption of during the acrylate monomers by cure and persists until the concentration gradient of monomer has disappeared. As more monomer is consumed, the concentration gradient disappears and the counter diffusion no longer drives the migration of LC molecules.

At this stage a second driving force for the migration of LC molecules is the polymer elasticity, known as 'hooping' stress, which is caused by the normal stress difference in two directions [26]. This hooping stress squeezes LC molecules out of the polymer phase and the ejected LC forms LC-rich streaks in the holograms. The hooping stress is directly related to the elasticity of urethane acrylate polymers which can be expressed in terms of the elastic modulus of rubber. According to rubber elasticity theory, the elastic modulus (G°_{N}) is given by [27]

$$G^{\circ}_{\mathrm{N}} = \frac{\rho R T}{Mc} \tag{2}$$

where ρ, R, T and M_{c} are the density, gas constant, absolute temperature and molecular weight between crosslinks, respectively. As the average functionality of the acrylate monomer increases, M_{c} of the acrylate domain decreases and ρ increases. These two factors contribute to an increase in elasticity of the polymer phase giving rise to the rapid squeezing of LC molecules. However, when the squeezing actions of the networks are too strong, with an excessively high average functionality, LC molecules are squeezed out so quickly they are subject to coalescence to give larger droplets and smaller droplet density, giving rise to a somewhat decreased diffraction efficiency [6]. Thus a maximum diffraction efficiency may exist, in relation to average monomer functionality.

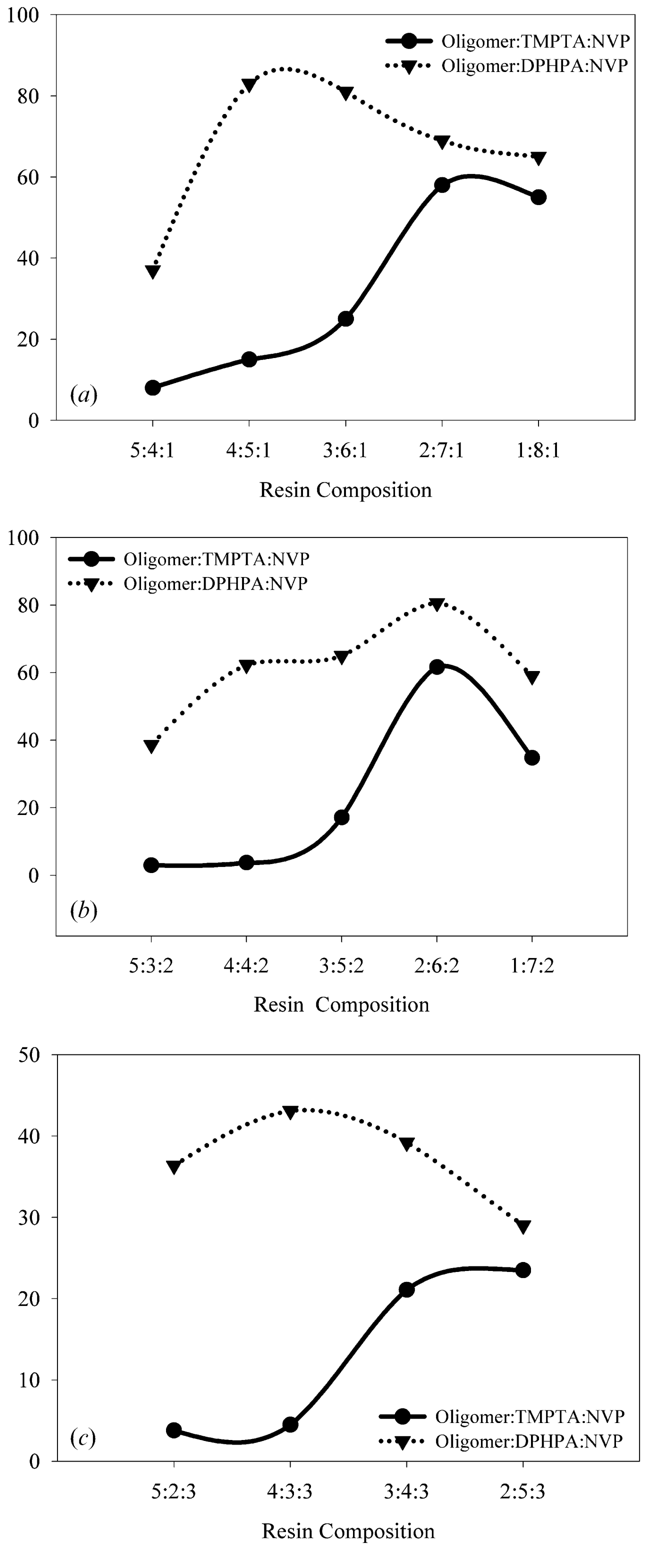

Figure 2. Diffraction efficiencies of the HPDLC films vs. various resin compositions (35 wt% LC, 50 mW cm^{-2}).

It is also of interest to see how the rate of network formation at a given final network density contributes to the grating formation. The effect of irradiation intensity has therefore been studied with a particular composition of pentacrylate(oligomer/DPHPA/NVP=4/5/1) where a maximum diffraction efficiency was obtained (figure 3). It can be seen that diffraction efficiency shows a maximum at 50 mW cm^{-2}, implying that an optimum rate of cure exists. Below this, network formation is insufficient to push the LC molecules out of the polymer phase, leading to insufficient grating formation; above this maximum the *in situ* formed elasticity of acrylate domains rapidly squeezes LC molecules out of the polymer phase, allowing coalescence which leads to large droplets with small droplet density. Large domains decrease diffraction efficiency and cause scattering [11].

A diffraction efficiency/laser intensity/LC content relationship is shown in figure 4. At low LC contents (25, 30, 35%), diffraction efficiency monotonically increases with irradiation intensity; at high LC contents (40, 45%) diffraction efficiency shows a maximum. It is also noted that high LC (low monomer) films are sensitive to low irradiation intensity, whereas low LC (high monomer) films are sensitive to high irradiation intensity. Perhaps the larger monomer content need requires greater irradiation energy for polymerization. Moreover, regarding the effect of LC content, maximum diffraction efficiency is obtained with 40% LC regardless of irradiation intensity. Below this concentration, the amount of LC is insufficient to form normal gratings, and above this the amount of polymer is insufficient for deep-support, and it is deformed [28]. As expected, diffraction efficiency monotonically increases with increasing cell gap, i.e. film thickness (figure 5). It

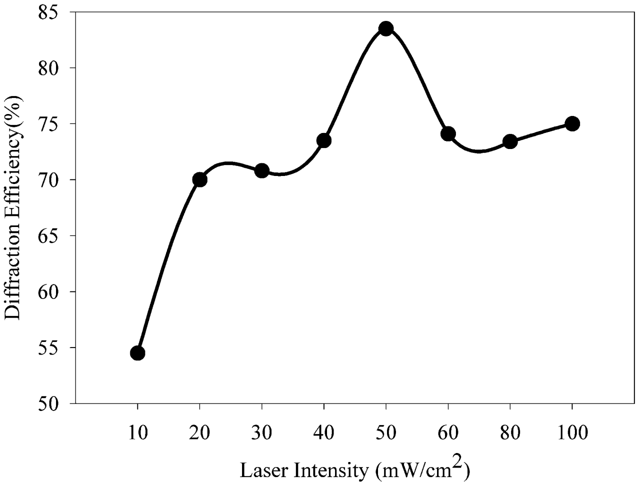

Figure 3. Diffraction efficiency vs. laser intensity (35 wt% LC, oligomer/DPHPA/NVP=4/5/1).

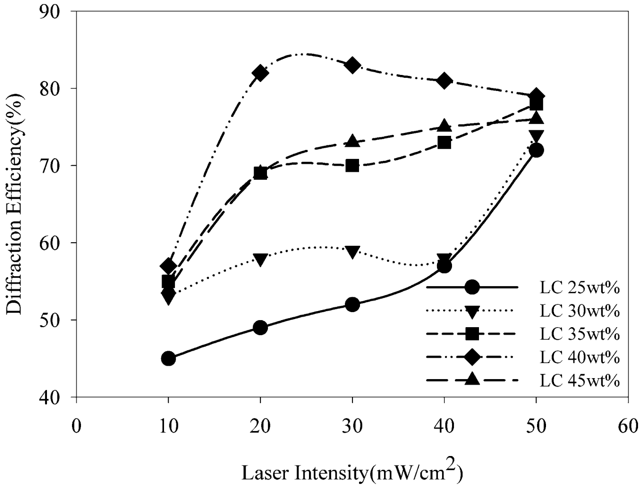

Figure 4. Diffraction efficiency vs. laser intensity vs. LC content (oligomer/DPHPA/NVP=4/5/1).

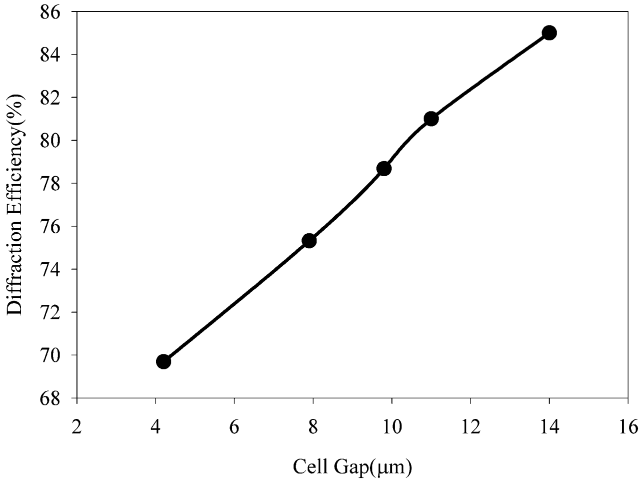

Figure 5. Diffraction efficiency vs. cell gap (35 wt% LC, 50 mW cm^{-2}, oligomer/DPHPA/NVP=4/5/1).

is also seen that the increase in diffraction efficiency is almost linear with film thickness, indicating that the grating is uniform along the thickness direction and absorption of light by the film is insignificant.

The angular selectivity and diffraction efficiency of composite films irradiated at various beam angles are shown in figure 6; corresponding SEM morphologies are given in figure 7 [29, 30]. Angular selectivity increases with increasing interbeam angle. With increasing interbeam angle, grating spacing decreases according to Bragg's law:

$$\lambda = 2d \sin \theta \tag{3}$$

where λ is the wavelength of incident light, d the grating spacing, and 2θ the interbeam angle outside of the film.

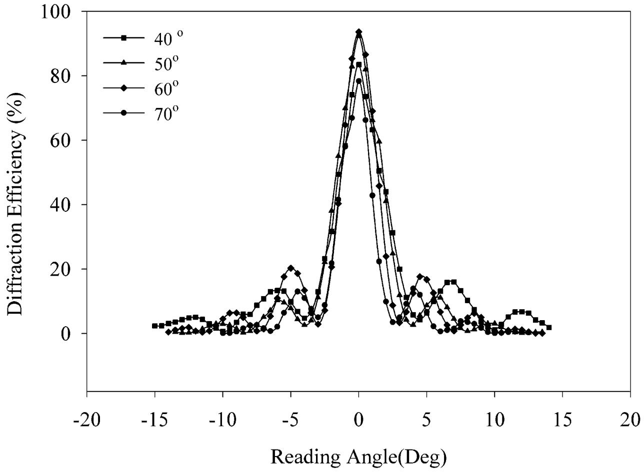

Figure 6. Angular selectivity of transmission hologram vs. various angles (35 wt% LC, 50 mW cm^{-2}, oligomer/DPHPA/NVP=4/5/1).

The increasing angular selectivity with increasing interbeam angle should arise from the small Bragg spacing where LC droplets are regular in size, giving a high diffraction efficiency and high angular selectivity [6]. However, when the interbeam angle is too large (70°), the grating spacing becomes too small and LC molecules are subjected to coalescence in LC-rich lamellae [11].

4. Conclusions

Diffraction gratings have been fabricated with polyurethane acrylates of different acrylate functionality with varying irradiation intensity, film composition, cell gap and reading angle. The diffraction efficiency shows a maximum in relation to the monomer composition(oligomer/multifunctional/monofunctional acrylate). However, regardless of the composition pentacrylate (DPHPA) gave a higher diffraction efficiency than triacrylate (TMPTA). This implies that network structure (i.e. crosslinking density) as well as the rate of cure play a significant role in grating formation and diffraction. The high elasticity of crosslinked domains probably effectively squeezes LC molecules out of the polymer phase. However, when the *in situ* elasticity formation is too strong, the squeezed LC molecules are likely to coalescence, leading to large droplets and poor diffraction efficiency.

The existence of an optimum irradiation intensity and LC content is related to the optimum rate of cure, which is balanced by the migration rate of LC molecules. A monotonic increase of diffraction efficiency with cell gap and interbeam angle confirms that the gratings are formed uniformly.

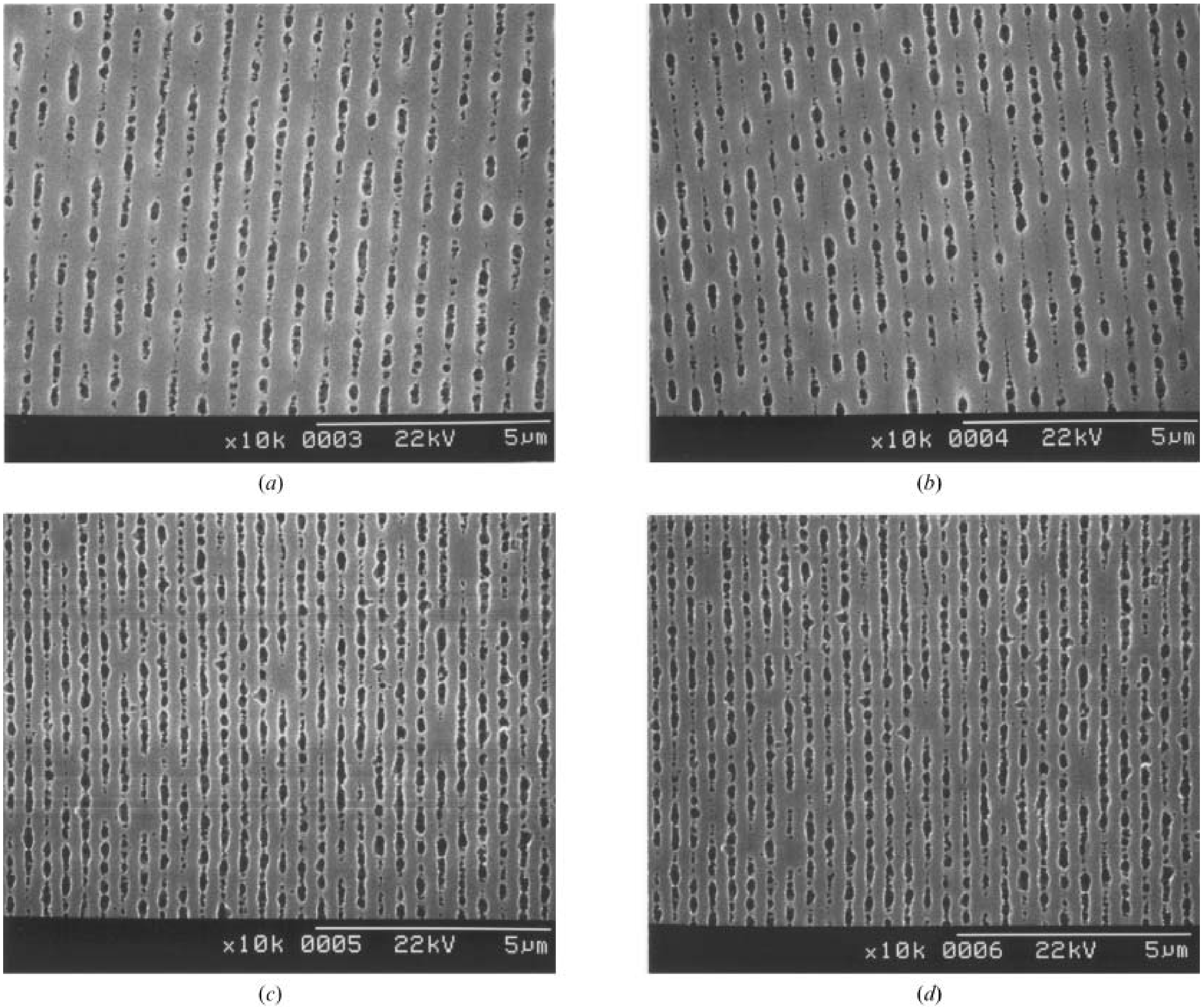

(*a*) (*b*) (*c*) (*d*)

Figure 7. Morphologies of the grating irradiation at various angles (35 wt % LC, 50 mW cm^{-2}, oligomer/DPHPA/NVP=4/5/1): (*a*) 40°, (*b*) 50°, (*c*) 60°, (*d*) 70°.

Acknowledgements

This research was supported by the Korea Ministry of Science and Technology (MOST) and Ministry of Information and Communication (MIC) via IMT2000.

References

[1] P.S. Drazaic. *Liquid Crystal Dispersions*. World Scientific, Singapore (1995).
[2] R.L. Sutherland, D.L. Vezie, W.W. Adams. *Polymer*, **36**, 2699 (1995).
[3] R.T. Pogue, R.L. Sutherland, M.G. Schmitt, L.V. Natarajan, S.A. Siwecki, V.P. Tondiglia, T.J. Bunning. *Appl. Spectrosc.*, **54**, 12 (2000).
[4] M. Mucha. *Prog. polym. Sci.*, **28**, 837 (2003).
[5] R.A. Vaia, D.W. Tomlin, M.D. Schulte, T.J. Bunning. *Polymer*, **42**, 1055 (2001).
[6] T.J. Bunning, L.V. Natarajan, V.P. Tondiglia, G. Dougherty, R.L. Sutherland. *Polym. Sci. polym. Phys.*, **35**, 2528 (1997).
[7] J.W. Doane, A. Golemme, J.L. West, J.B. Whitehead, B.G. Wu. *Mol. Cryst. liq. Cryst.*, **165**, 511 (1988).
[8] T.J. Bunning, L.V. Natarajan, V.P. Tondiglia, R.L. Sutherland. *Ann. Rev. mater. Sci.*, **115**, 83 (2000).
[9] M. Date, Y. Takeuchi, K. Tanaka, K. Kato. *Proc SID*, **7**, 17 (1999).
[10] M. Date, Y. Takeuchi, K. Tanaka, K. Kato. *Ieice. Trans. Electron.*, **E81-C**, 1685 (1998).
[11] K. Kato, K. Tanaka, M. Date. *Electron. Commun. Jap. 2*, **81**, 32 (1998).
[12] H.F. Mork. *Opt. Lett.*, **18**, 915 (1993).
[13] D.H. Shin, J.S. Jang. *Appl. Opt.*, **37**, 329 (1998).

[14] Y.H. Cho, B.K. Kim. *J. polym. Sci. polym. Phys.*, **36**, 1393 (1998).

[15] Y. Miyamoto, H. Kikuchi, Y. Morimura, T. Kajiyama. *New polym. Mater.*, **2**, 1 (1990).

[16] G. Odian. *Principles of Polymerization*. John Wiley, New York (1981).

[17] C.F. Nostrum, R.J.M. Nolte. *Chem. Mater.*, **10**, 135 (1998).

[18] G.H. Zhao, P. Mouroulis. *J. mod. Opt.*, **41**, 1929 (1994).

[19] G.M. Karpov, V.V. Obukhovsky, T.N. Smirnova, V.V. Lemeshko. *Opt. Commun.*, **174**, 391 (2000).

[20] S.H. Kim, B.K. Kim, J.C. Song. *Polymer*, **39**, 949 (1998).

[21] K. Mar, R.T. Pogue, L.V. Natarajan, S.A. Siwecki, V.P. Tondiglia, R.L. Sutherland, T.J. Bunning. *Polymer*, **41**, 733 (2000).

[22] M.D. Sarkar, N.L. Gill, J.B. Whitehead, G.P. Crawford. *Macromolecules*, **36**, 630 (2003).

[23] C. Serbutoviwz, J.G. Kloosterboer, H.M. Boots, F.J. Touwslager. *Macromolecules*, **29**, 7690 (1996).

[24] V.L. Colvin, R.G. Larson, A.L. Harris, M.L. Schilling. *J. appl. Phys.*, **81**, 5913 (1997).

[25] R.B. Bird, W.E. Stewart, E.N. Lightfoot. *Transport Phenomena*. Wiley, New York (1960).

[26] R.B. Bird, R.C. Armstrong, O. Hissager, C.F. Curtiss. *Dynamics of Polymeric Liquids*. John Wiley, New York (1977).

[27] A.N. Gent. *Engineering with Rubber*. Hanser, New York (1992).

[28] Y.J. Liu, B. Zhang, Y. Jia, K.S. Xu. *Opt. Commun.*, **218**, 27 (2003).

[29] S. Harbour, T. Galstian, R.S. Akopyan, A.V. Galstyan. *Opt. Commun.*, **238**, 261 (2004).

[30] R.S. Akopyan, A.V. Galstyan, T.V. Galstian. *J. Exp. theor. Phys.*, **99**, 101 (2004).